Journal of the Korean Magnetic Resonance Society **2005**, *9*, 1 - 20

The V(IV) Species, Location and Adsorbate Interactions in VH-SAPO-11 studied by ESR and ESEM

Gernho Back [1*], Seung-Chan Baek [2], Sung-Gun Park [1*], and Chul Wee Lee [2]

[1] Department of Chemistry, Changwon National University, Changwon, Kyungnam, 641-773, Korea
[2]Advanced Chemical Technology Division, KRICT, Daejon 305-606, Korea
Received December 3, 2004

Abstract : Vanadium-incorporated aluminophophate molecular sieve VH-SAPO-11 has been studied by electron spin resonance (ESR) and electron spin echo modulation (ESEM) spectroscopies to determine the vanadium location and interaction with various adsorbate molecules. As-synthsized VH-SAPO-11 contains only vanadyl species with distorted octahedral coordination. After calcinations in O_2 and exposure to moisture, only species A is observed with reduced intensities. Species A is suggested as a $VO(H_2O)_2^{2+}$ complex coordinate to three framework oxygen bonded to aluminum. When calcined, hydrate VH-SAPO-11 is dehydrated at elevated temperature, species A loses its water ligands and transforms to VO^{2+} ions coordinated to three framework oxygens (species B). Species B reduces its intensities significantly after treatment with O_2 at high temperature, thus suggesting oxidation of v^{4+} to v^{5+}. When dehydrated VH-SAPO-11 contacts with D_2O at room temperature, the ESR signal of species A is observed. This species assumed as a $VO(O_f)_3(D_2O)_2$, by considering 3 framework oxygens. Adsorption of deuterated methanol on dehydrated VH-SAPO-11 results in another new vanadium species D, which is identified as a $VO(CD_3OH)$ complex. When deuterated ethanol is adsorbed on dehydrated VH-SAPO-11, another new vanadium species E identified as a $VO(C_2H_5OD)^{2+}$, is observed. When deuterated propanol is adsorbed on dehydrated VH-SAPO-11, a new vanadium species F identified as a $VO(C_3H_7OD)$, is observed. Possible coordination geometries of these various complexes are discussed.

Keywords: V(IV), VH-SAPO-11, ESR, ESEM

INTRODUCTION

Various microporous crystalline aluminophosphates ($AlPO_4$-N) have been synthesized

* To whom correspondence should be addressed. E-mail: ghback@changwon.ac.kr

hydrothermally with isopropylamine being used as the templating agent. These structures have a three-dimensional microporous crystal framework arrangement of SiO_4, PO_4 and AlO_4 tetrahedral connected through the shared oxygen atoms.[1-2]. A serious defect of these materials with respect to catalytic potential is the lack of Brönsted acidity due to the neutrality of their frame.[1] Mechanically, we can consider their composition in terms of silicone substitution into hypothetical aluminophosphate frameworks. First, the substitution can occur via replacement of one framework aluminum by silicon and second, the replacement of phosphorus by silicon or the simultaneous substitution of one aluminum and one phosphorus by two silicon. According to the substitution mode, the net framework charge per silicone framework atom would be +1, -1, 0, respectively.[3]

The preliminary studies on SAPO materials show that the silicone substitutes via second and third mechanisms.[4-6] They exhibited the property of the zeolite and aluminophophate and moreover, exhibit various specific properties, such as adsorbents for separation and purification of molecular sieves, catalyst, or catalyst supports and ion-exchanged agents. The framework phosphorus substitution by silicon is a consequence of the fact created a net negative framework charge, which is compensated by exchangeable ion which are usually protons after calcination. The fact that H^+ ion can be ion-exchanged partially by transition metal ion makes SAPO materials interesting candidate for various catalytic reactions.[6]

Vananadium incorporated silica molecular sieves (e,g., VS-1, VS-2, VMCM-41, etc) and aluminophosphate molecular sieves (e. g., VAPO-5, VAPO-11, etc) exhibit catalytic activity in several oxidation and ammoxidation reaction.[7-8] It is well-known that the catalytic properties of transition metal incorporated molecular sieves are strongly dependent on the nature and location of the metal ions and on their accessibility and coordination with adsorbate molecules. The nature of vanadium in VAPO-5 has been studied by combining various spectroscopic methods.[9-10] Oxidation state of vanadium in the final product largely depends on vanadium source used. The vanadium is mostly found as V^{4+} when vanadyl sulfate or V^{4+}-containing solution is used as a vanadium source. However, both V^{4+} and V^{5+} are found in VAPO-5 when V_2O_5 is used, which suggests that some V^{5+} is reduced to V^{4+}

during the gel preparation or crystallization process.[9]

The incorporation of vanadium during hydrothermal synthesis of SAPO-11 is reported. The studies on structure of vanadium in VAPSO-11 have been perfomed by ESR, ^{51}V NMR and the other spectroscopic methods. They revealed that vanadium in VAPSO-11 is located in square pyramidal or distorted octahedral structure. Vanadium shows redox behavior (V^{4+} to V^{5+} and vice versa) when calcined and reduced.[10]

In a recent report we have shown the location and adsorbate interactions of V(IV) species in VH-SAPO-34. That study illustrated that the V(IV) species exist as a vanadyl ion either as $[V(IV)]O^{2+}$ or V^{4+}, a conclusion which is somewhat unclear that the V(IV)species seem to be more probable because SAPO-34 having a low negative framework charge[11]. While ESR can be used to deduce the local symmetry of the transition metal ions, analyses of the ESEM signals yield the number and coordination distance of associated ligands. However, ESEM spectroscopy has not been used so far to characterize vanadium-doped SAPO-11, there has been a few published paper to characterize the structure of V(IV) in silicoaluminophosphate molecular sieves clearly. In this work, vanadium-doped H-SAPO-11 samples were prepared by a high-temperature solid-state reaction between SAPO-11 and V_2O_5 and characterized, we describe ESR and ESEM studies on VH-SAPO-11 to achieve information on the nature, location, and adsorbate interactions of vanadium in this material.

EXPERIMENTAL SECTION

Preparation

Synthesis and Solid-state ion exchange of SAPO-11 were carried out by a modification of the reported methods in the literatutre.[11] An aqueous solution (9.19125 g) of aluminum isopropoxide(Aldrich) was prepared, after adding 13.0 ml of de-ionized water to 9.19125 g of aluminum isopropoxide, homogenizing by hand with continuous stirring and stirred for 1 hour at room temperature. Then, 5.1279 g of 85 wt % H_3PO_4 was added by drop by drop to

this solution while the temperature is controlled with an ice bath at 273 K and stirred at 273 K for 15 min and stirred at 298 K for 1 hour. To this solution were added 1.0013 g of 30 wt % SiO_2 and 1.0 ml of H_2O successively drop by drop with mixing for 30 min. Then, 2.5553 g of *i*-Pr_2NH was added drop by drop. And the solution aged at room temperature for 24 h to form a gel. The gel was sealed in a stainless steel pressure vessel lined with Teflon and heated in a oven at 493 K for 5 days. This solid reaction product was collected by filtration, washed with distilled water, and dried in air at 373 K. This product is called "as-synthesized" H-SAPO-11.

VH-SAPO-11, in which V(IV) ions are in extra-framework positions, was prepared by solid-state ion exchange using V_2O_5 and H-SAPO-11. A mixture of 0.010 g of vanadium oxide and 0.5 g of H-SAPO-11 was ground in a mortar with a pestle for 30 min. This solid mixture was then heated in an oven at 773 K in O_2 for 2 h and slowly cooled to room temperature. Before and after solid-state ion exchange, the sample remained white. The idealized chemical composition of this sample was $V_{0.003}H_{0.024}(Si_{0.07}Al_{0.48}P_{0.45})$ based on electron probe microanalysis.

Sample Treatment and Measurement

The V ion-exchanged and calcinations of as-synthesized SAPO-11 were examined by the use of a powder X-ray diffraction(XRD) with a Phillip PW 1840 diffractometer using Cu K_α radiation. Thermogravimetric analysis was performed by a Dupon 951 thermal analyzer with heating rate of 10℃ min^{-1}. Chemical analysis of the samples were carried out by electron microprobe analysis o a JEOL JXA-8600 spectrometer. A hydrated VH-SAPO-11 was first loaded into 3 mm out diameter by 2 mm inner diameter. Calcined and hydrated VH-SAPO-11 was examined by ESR without any pretreatment. This sample was then evacuated to a final pressure of 10^{-4} Torr at room temperature overnight. To study redox behavior of VH-SAPO-11, evacuation was continued by raising the temperature slowly to 773 K and then contacted with 1 atm of O_2 at 843 K for 18 h, cooled to room temperature to give a oxidized sample (Note the EPR spectrum Fig. 3c). To study the ESR behavior of the

vanadium as a function of dehydration this sample was heated under vacuum and maintained at this temperature for 18 h(Fig. 3 b). To study vanadium interaction with various adsorbates, dehydrated VH-SAPO-11 samples were exposed to the room-temperature vapor pressure of D_2O (Aldrich Chemical), CD_3OH, CH_3OD, C_2H_5OD, $CH_3CH_2CH_2OD$ from Cambridge Isotope Laboratories. These samples with adsorbates were sealed and kept at room temperature for 24 h before ESR and ESEM measurements.

The ESR spectra were recorded with a modified Varian E-4 spectrometer interfaced to a Tracer Norton TN-1710 signal averager at 77 K. Each spectrum was obtained by multiple scan to achieve a satisfactory signal-to-noice-rate. Each acquired spectrum was transferred from the signal averager to an IBM PC/XT compatible computer for analysis and plotting. The magnetic field was calibrated with a Varian E-500 gauss meter. ESEM spectrum was measured at 4 K with a Bruker ESP 380 pulsed ESR spectrometer. Three pulse echoes were measured by using a 90 °-τ-90 °- T –90 ° pulse sequences with τ = 0.26~0.28 μs and echo intensities was measured as a function of T. The theory and simulation of ESEM are described elsewere.[12]

RESULTS

VH-SAPO-11 samples were characterized by powder X-ray diffraction (XRD), which confirmed the crystallinity and phase purity. The observed XRD pattern, both in intensities and line position, matched with the pattern reported for the AEL structure type(Fig. 1).[13]

Practically no loss in crystallinity was observed when the as-synthesized sample was calcined by heating with O_2 at 773 K for 3.5 h to remove the organic template. The chemical composition of VH-SAPO-11 was examined by electron probe microanalysis. Composition were analyzed for a number of crystals. An approximate chemical composition sample is found to be $[V_{0.003}H_{0.024}(Si_{0.07}Al_{0.48}P_{0.45})]$. Before calcinations and after calcinations the colour of the VH-SAPO-11 was white. Thermal analysis of VH-SAPO-11 is shown in Fig. 2. Thermoanalytical curves of VH-SAPO-11 reveal that calcinations process under air

proceeds in five stages, as in case of MeAPSO-11.[14] Stage I shows endothermic desorption of water. Stage II-V shows the oxidative decomposion of the template molecules and in all these stages, exothermic peaks are measured. For SAPO-11 the removal of the template under stage IV and V is extremely weak. The main process of the decomposition of the template proceeds in stage II and III. The ESR spectrum of the calcined and hydrated VH-SAPO-11 is shown in Fig. 3a.

The spectrum ia similar to VAPSO-11 reported earlier,[10] and characterized by axially symmetric signal designated here as species A with hyperfine structure. The ESR parameter is $g_{\|} = 1.927$ and $A_{\|} = 180 \times 10^{-4}$ cm^{-1} for species A. This parameters are typical of V^{4+} in a vanadyl environment with distorted octahedral coordination.[15-17] The spectrum shows hyperfine structure due to interactions of the unpaired $3d^1$ electron with the ^{51}V nucleus whose spin is 7/2 and which is present in 99.76 % abundance.

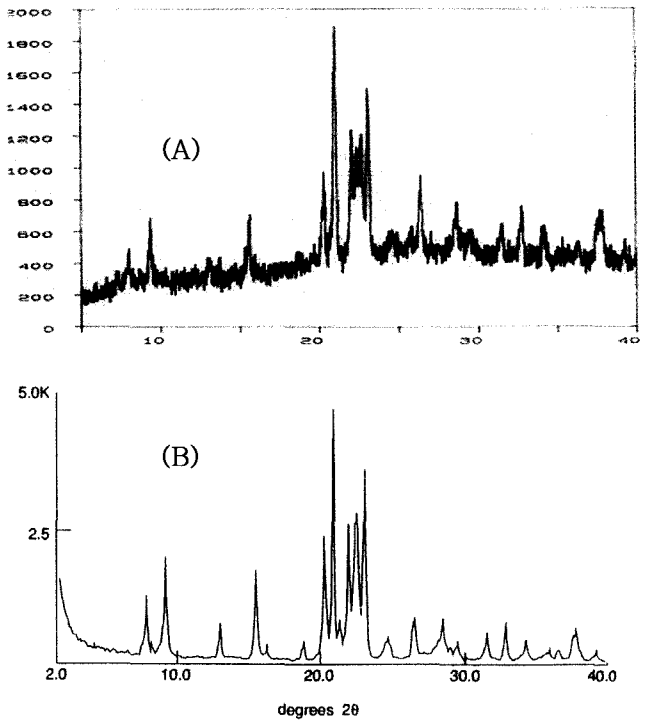

Fig. 1. XRD patterns of synthesized samples (A) SAPO-11[13], (B) H-SAPO-11.

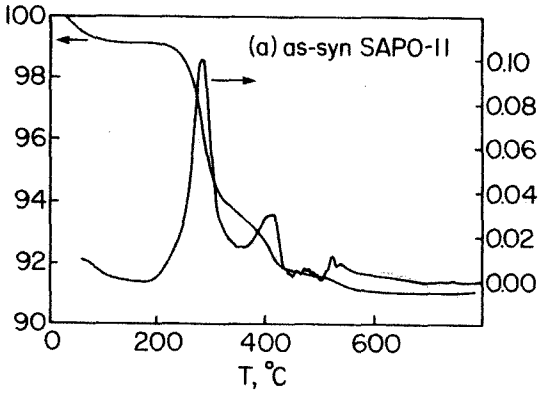

Fig. 2. DTA patterns of as-synthesized samples SAPO-11.

Another feature of these signals are the unequal separations of the various hyperfine lines due to second-order effects. The extend of this variation can be seen, for example, in signal A where $A_{\perp}$ varies from 51 x 10^{-4} cm^{-1} to 86 x 10^{-4} cm^{-1} in going from the first two line on the low-field side to the final two line on the high-field side. The well-resolved hyperfine structure suggests a high dispersion of VO^{2+} ions in VH-SAPO-11. Moreover, the observed ESR spectrum has a horizontal baselines and no superimposed broad signal, which indicates that polymeric nuclear V^{4+} species are absent in VH-SAPO-11. Also. The V^{4+} content of as-synthesized VH-SAPO-11 estimated from double-integrated ESR specra is the same magnitude as the vanadium content obtained by chemical analysis. This supports the assumption that no polynuclear oxidic vanadium is present in our sample.

The ESR spectrum of calcined, hydrated VH-SAPO-11 is evacuated at room temperature overnight , the resultant spectrum differs considerably from that of calcined, hydrated sample(not submitted). The changes are more pronounced upon dehydration of a sample at high temperatures. And after dehydration of a sample at high temperature, and after dehydration at 843 K a single new vanadium species B is observed in the spectrum (Fig. 3b) The ESR parameters of species B are $g_{\|}$ = 1.907 and $A_{\|}$ = 180 x 10^{-4} cm^{-1}. Species B remains in the spectrum (Fig. 3c), although with less intensities, after treatment with O_2 at 843 K for 18 h.

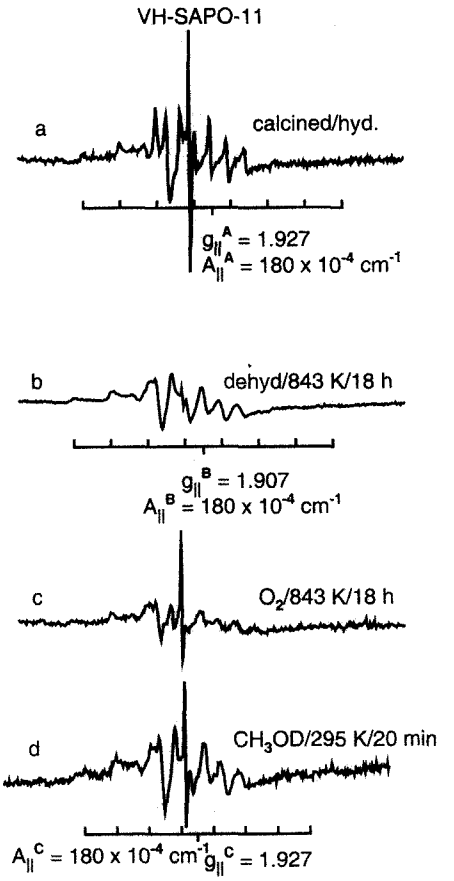

Fig. 3. ESR spectra at 77 K of VH-SAPO-11; (a) calcined, hydrated sample, (b) after ~ 18 h evacuation at 843 K, (c) contacted with O_2 for 18h at 843 K, (d) adsorbed with CH_3OD for 20 min at 295 K.

The intensities of species B is about 1/5 the intensities of the intensity of the as-synthesized VH-SAPO-11. This shows that a significant part of V^{4+} is oxidized to V^{5+}.

Fig. 3d and Fig. 4 show the ESR spectra observed when CH_3OD, CD_3OH, CH_3CH_2OD, $CH_3CH_2CH_2OD$ and D_2O are adsorbed on dehydrated VH-SAPO-11 samples at room temperature. A single vanadium species with ESR parameters the same as species A observed in adsorbed by D_2O or calcined, hydrated VH-SAPO-11(Fig. 3d). This suggests

that species A is an aquo-vanadyl complex. The ESR spectrum recorded on VH-SAPO-11 after adsorbing CH_3OD shows a new vanadium species C characterized $g_{\|} = 1.927$ and $A_{\|} = 180 \times 10^{-4}$ cm^{-1}. The ESR spectrum recorded on VH-SAPO-11 after adsorbing CD_3OH shows a new vanadium species D characterized by $g_{\|} = 1.917$ and $A_{\|} = 183 \times 10^{-4}$ cm^{-1}. When deuterated ethanol is adsorbed on dehydrated VH-SAPO-11 at room temperature, a new vanadium species E with parameters $g_{\|} = 1.918$ and $A_{\|} = 183 \times 10^{-4}$ cm^{-1} is observed (Fig. 4b).

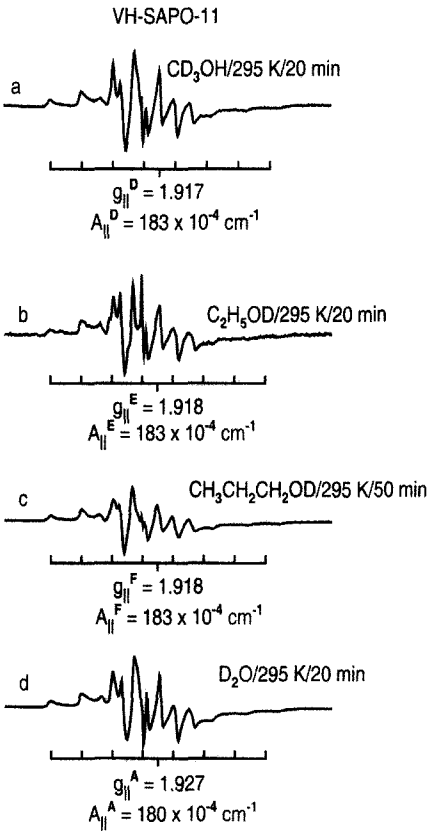

Fig. 4. ESR spectra at 77 K of VH-SAPO-11; (a) adsorbed with CD_3OH for 20 min at 295 K, (b) adsorbed with C_2H_5OD for 20 min at 295 K, (c) adsorbed with C_3H_7OD for 50 min at 295 K, (d) adsorbed with D_2O for 20 min at 295 K.

Another new vanadium species F characterized by $g_{\|} = 1.918$ and $A_{\|} = 183 \times 10^{-4}$ cm^{-1} is observed when deuterated propanol is adsorbed on dehydrated VH-SAPO-11 at room temperature (Fig. 4c). The observed ESR parameters and possible assignments of the various vanadium species investigated are summarized in Table 1.

Table 1. ESR Parameters at 77 K of Paramagnetic Ion Species, Pd(I) and V(IV) after Various Adsorbate Treatments in H-SAPO-11

	PdH-SAPO-11[27]			VH-SAPO-11[A]	
treatment Activated Species: adsorbate Site	$g_{\|}$ g_1 g_2	$g_{\perp}$ g_3	activated species: adsorbate Site	$g_{\|}$	$g_{\perp}$
Pd^+	2.642	2.132			
Pd^+	2.942	2.132	$VO(O_f)_3$: I	2.09	1.970
Pd^+-$(H_2O)_2$	2.073 2.031	1.996	$VO(O_f)_3(D_2O)_2$: II_1^*	1.927	1.990
Pd^+-(CD_3OH)	2.620	2.104	$VO(O_f)_3(CD_3OH)$: II_1^*	1.917	1.982
			$VO(O_f)_3(CH_3OD)$: II_1^*	1.927	1.990
			$VO(O_f)_3(C_2H_5OD)$: II_1	1.918	1.983
			$VO(O_f)_3(C_3H_7OD)$: II_1	1.927	1.984

[A]: present work

Three-pulse ESEM spectra were recorded at 3380 G at a microwave frequency of 9.808 GHz for various VO^{2+} species. The echo signal was found to be a maximum around this field. $^2D(I = 1, \nu = 2.288$ MHz, 99.8 %) nucleus was investigated for spin echo modulation. For a particular nucleus, the delay between the first and second pulses (τ) was selected to minimize modulation from other magnetic nuclei present in the system. Fig. 5b are the experimental and simulated ^2D ESEM spectra of VH-SAPO-11 after adsorbing CH_3OD. The interpulse time τ was selected as 0.26 μs. Simulation of the spectrum gives one deuterium at

2.9 Å. This value is consistent with one CH_3OD molecule coordinating directly with V^{4+} ions in species C. Fig. 5a shows the experimental and simulated ^2D ESEM spectra of VH-SAPO-11 after CD_3OH adsorption. The magnetic field and τ values are the same as for CH_3OD. Simulation of the spectrum gives three deuteriums at 3.5 Å. These parameters are consistent with one CD_3OH molecules coordinating with V^{4+} ions in species D. Fig. 6a. shows the experimental and simulated ^2D ESEM spectra for VH-SAPO-11 after adsorbing CH_3CH_2OD. Simulation of the spectrum gives one deuterium at 3.9 Å. These parameters are consistent with one CH_3CH_2OD molecule coordinating with V^{4+} ions in species E. Fig. 6b. shows the experimental and simulated ^2D ESEM spectrum observed for VH-SAPO-11 after adsorbing $CH_3CH_2CH_2OD$. The spectrum is simulated with one deuterium at 4.2 Å. These parameters can be rationalized in terms of one propanol coordinating with V^{4+} ions in species F. The observed ESEM parameters of the vanadium species investigated are summarized in Table 2.

Table 2. ESEM parameters for V(IV) with various adsorbates in H-SAPO-34 and H-SAPO-11

	PdH-SAPO-11[27]			VH-SAPO-11[a]		
adsorbate	N[a]	R[b]	A(MHz)[c]	N[a]	R[b]	A(MHz)[c]
D_2O	4	0.37	0.20			
CD_3OH	3	0.40	0.01	3	0.35	0.10
CH_3OD				1	0.292	0.14
CH_3CH_2OD				1	0.388	0.23
$CH_3CH_2CH_2OD$				1	0.42	0.23

[a]Number of deuterium nuclei. [b]Distance between V(IV) and deuterium; estimated uncertainty is ±0.01nm. [c]Isotropic hyperfine coupling constant; estimated uncertainty is ±10%. [a]this work.

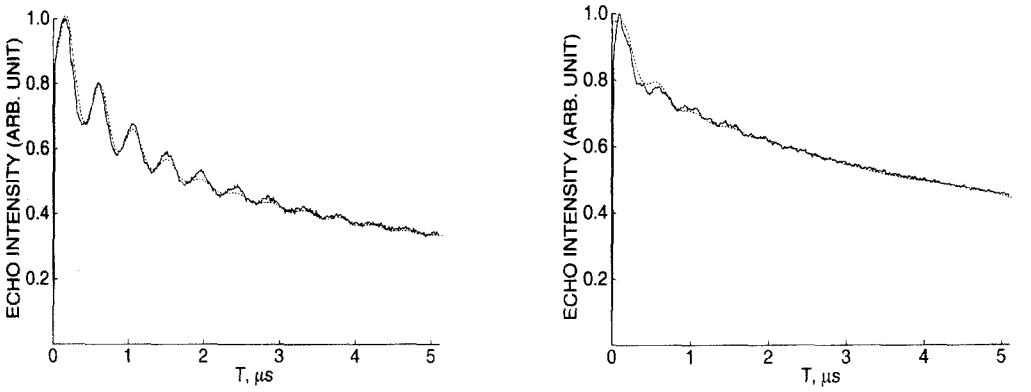

Fig. 5. Experimental(-) and simulated(---) three pulse ESEM spectra at 4 K of activated VH-SAPO-11 with (a) CD_3OH (N=3, R=0.35 nm, A=0.10 MHz) and (b) CH_3OD (N=1, R=0.292 nm, A=0.14 MHz).

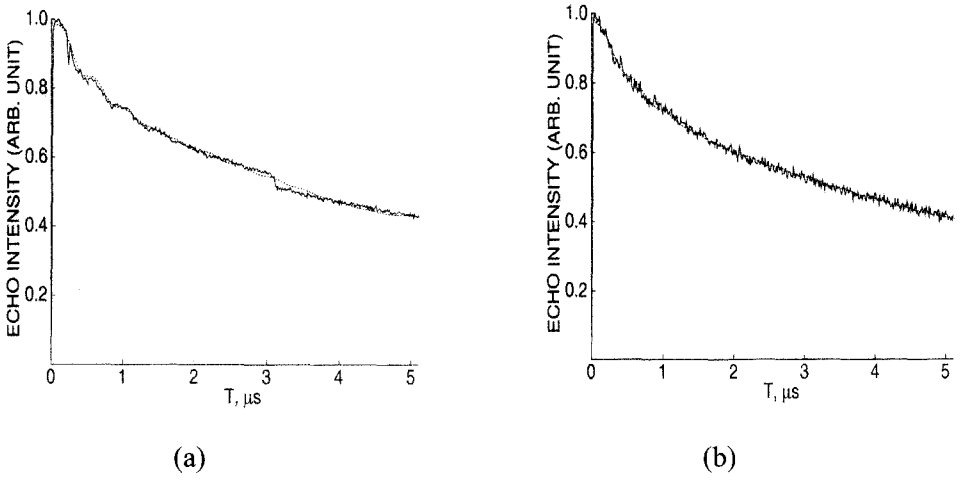

Fig. 6. Experimental(-) and simulated(---) three pulse ESEM spectra at 4 K of activated VH-SAPO-11 with (a) CH_3CH_2OD (N=1, R=0.388 nm, A=0.23 MHz) (b) $CH_3CH_2CH_2OD$ (N=1, R=0.42 nm, A=0.23 MHz).

DISCUSSIONS

Vanadium(IV) normally enters into compound as oxovanadium(IV) commonly called a "vanadyl" entity VO^{2+} and exhibits paramagnetic resonance absorption due to a single unpaired electron. The electronic state of VO^{2+} ion is normally dependent on the $3d^1$ electron of vanadium and therefore, the levels of VO^{2+} are similar to those of the V^{4+} ion. When a vanadyl ion is incorporated into a crystal lattice by coordination with other ligands, it is subjected to a crystalline field due to the surrounding environment. The most common coordination of vanadium is octahedral or square pyramidal often with tetragonal distortion. The electronic structures of two vanadyl species for as-synthesized VAPO-5 were described by Prakish and Kevan[18], where vanadium ion is an distorted octahedral coordination (Table 3).

On the basis of a LCAO-MO model, it has been shown that the unpaired electron occupies a nonbonding b_2 type of vanadium orbital($3d_{xy}$) and that the lowest state becomes an orbital singlet. The ESR spectra of VO^{2+} are complicated by the high number of hyperfine levels generated due to magnetic interaction with the vanadium nucleus and by second effects that tend to produce an asymmetric hyperfine structure with unequal separation of the various lines.

The electronic absorption spectrum reported for VAPSO-11 shows two absorption bands at 280 nm and 500-800 nm.[10] Moreover, the ESR parameters of VO^{2+} in VAPSO-11 are camparable to corresponding values in compounds where VO^{2+} has octahedral with tetragonal distorsion. Thus, it is likely that species A in calcined, hydrated VH-SAPO-11 are due to VO^{2+} in distorted octahedral environment whereas species A is observed in calcined, hydrated VH-SAPO-11 and also in dehydrated VH-SAPO-11 after adsorption of D_2O. In the latter case, we do not achieve any other the ^2D ESEM spectrum. But, it seems to be two water molecules due to the following reason. Thus to attain octahedral symmetry, v^{4+} ion has to coordinate two water and three more oxygens from the framework.

Table 3. Comparison of Spin Hamiltonian Parameters of VO^{2+} in Several Matrices

System	vanadium species	site symmetry	T(K)	$g_{\parallel}$	$g_{\perp}$	$^{a}A_{\parallel}$	$^{a}A_{\perp}$	Ground state	ref
VH-SAPO-11	VO^{2+}	Octahedral	300	1.927	1.990	180	79	d_{xy}	PW
VAPSO-11	VO^{2+}	Octahedral	300	1.925	1.993	184	67	d_{xy}	10
GeO_2 amorphous	VO^{2+}	Octahedral	300	1.929	1.976	75	68	d_{xy}	26
$VOPO_4 2H_2O$	VO^{2+}	Octahedral	300	1.938	1.976	75	64	d_{xy}	23, 24
V_2O_5/TiO_2	VO^{2+}	Octahedral	77^{++}	1.909	1.936	70	-	d_{xy}	22
V_2O_5/SiO_2	VO^{2+}	Octahedral	300	1.941	1.996	79	70	d_{xy}	25
V_2O_5/Al_2O_3	VO^{2+}	Octahedral	300	1.946	1.987	177	69	d_{xy}	25
$VOSO_4$/SAPO-34	VO^{2+}	Octahedral	300	1.906	2.016	191	86	d_{xy}	11
V_2O_5/SAPO-34	VO^{2+}	Octahedral	300	1.905	2.015	191	85	d_{xy}	11

[a]Units of 10^{-4} cm^{-1}
[++]Spectrum can also be observed at 300 K.
References : PW : Present work

The presence of A species indicates that there are at least two different location for vanadyl ion in activated VH-SAPO-11 molecular sieve. The previous paper[19] reported three sites for Cu(II) in CuH-SAPO-11 and suggested site II* as the most accessible, site II as intermediately accessible and site II' as the lest accessible.[20] Thus v^{4+} has to coordinate three more oxygens from site II (Fig. 7.).

The observed ESEM results on VH-SAPO-11 support the model suggested by Montes et al.[15] Wherein the vanadyl species neutralize partially three Al-O^- groups from the framework$^+$ due to vanadyl species existed in extra-framework, leaving one additional Al-O^- to be neutralized by protonated templated species or by H_3O^+.

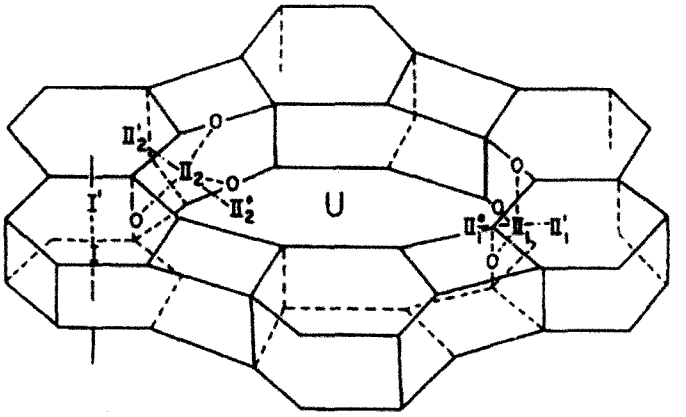

Fig. 7. Simplified structure of SAPO-11, showing possible cation positions. See text for description of the cation positions.[19]

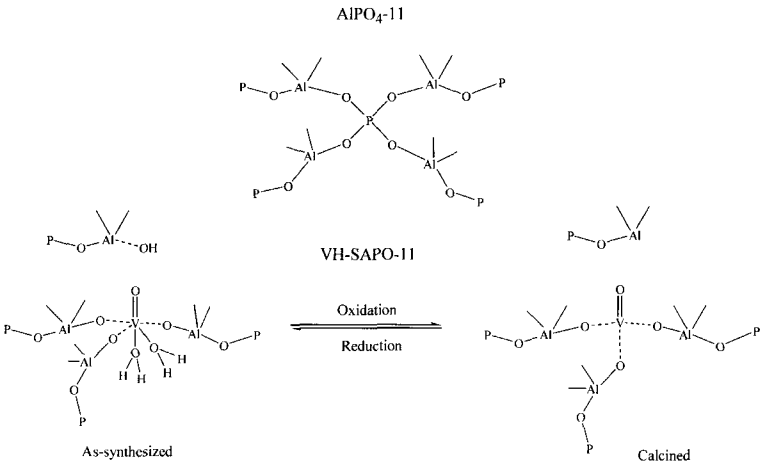

Fig. 8. Possible structure of vanadium species in as-synthesized and calcined VH-SAPO-11 contrasted with the structure of $AlPO_4$-11.

The low intensities of species A observed in calcined, hydrated VH-SAPO-11 is indicative of oxidation of some of the V^{4+} ion to V^{5+} ion during calcinations in O_2. Upon

evacuation of calcined, hydrated VH-SAPO-11, the ESR spectrum changes significantly. And finally, after dehydration at 773 K, a new species B is observed. Species B is probably VO^{2+} with no water or hydroxyl ligands and coordinated with only framework oxygens. The observation that species A changes to species B by evacuation at elevated temperature and species B returns to species A again after adsorption of D_2O is strong indication of the hydrated nature of species. As a results of this, the local symmetry of V^{4+} ions may be different for these two species. The reduction in intensities of B compaired to species A after O_2 treatment at 843 K is probably due to oxidation of some of the V^{4+} ions to V^{5+}. Although the ESR parameters of these species are characteristic of the vanadyl ion, the exact nature of the vanadium species is unclear. Species B has lower g and A values. The change in the g value is an indication of a change in the environment. The observed values of species B there propose tetrahedral symmetry for the V^{4+} ion. Tetrahedral V^{4+} ion has been suggested earlier in MFI vanadium silicate molecular sieve after reduction.[20] A possible model that is consistent with our various observations on the location and redox behavior of vanadium in VH-SAPO-11 is shown in Fig. 8.

Although several studies have been carried out on the nature of vanadium, especially its oxidation state and location in molecular sieves, studies on the interaction of this ions with external adsorbates are limited. To study the redox behavior of vanadium incorporated in APSO-11, these materials have been studied by ESR and ^{51}V NMR. They reported that on calcinations, V^{4+} species are converted to V^{5+} species. In the present study, the fact that the ESR parameters of VO^{2+} changes significantly after adsorption of various molecules indicates direct insertion of these molecules into the first coordination sphere of vanadium ion. This is further confirmed by the ^{2}D ESEM spectra observed for these complexes.

Adsorption of CD_3OH on dehydrated VH-SAPO-11 generates a new species D with ESR parameters different from those of species B. ^{2}D ESEM results of one deuterium interacting at 3.5 Å and is consistent with the coordination of one methanol molecules to the V^{4+} ion. This suggests that the immediate coordination sphere of V involves O ligands. The first coordination sphere of the vanadium species C involves only oxygen ligands from both

framework and the methanol molecules. Species C is therefore most likely a square pyramidal complex compared to the octahedral symmetry observed for species A. This difference in symmetry may account for the observed difference in the ESR parameters for species D compared to species A. Adsorption of CD_3OH on VH-SAPO-34 generates a complex in which one methanol molecule coordinates with VO^{2+} ions.[11] In CuH-SAPO-11, only two molecules methanol are found to coordinate with the first coordination sphere of the Cu^{2+} ions.[19] Similarly, when methanol is adsorbed on PdK-L, one molecule of methanol coordinates with the Pd ion.[24] It should be noted that unlike Cu^{2+} ion present in the extra-framework of CuH-SAPO-11, VH-SAPO-11 contains the VO^{2+} ion, which includes a vanadyl oxygen, incorporated into the extra-framework. Thus, the presence of vanadyl oxygen and its orientation inside the channel are factors that may influence the formation and nature of various metal-adsorbate complexes in VH-SAPO-11.

With adsorbed CH_3CH_2OD, VH-SAPO-11 shows a new vanadium species E. ^2D ESEM parameters of one deuterium at 3.9 Å is consistent with one ethanol molecule coordinating with V^{4+}. Fig. 9. shows a schematic of one ethanol molecule and three lattice oxygens from six-ring window around V^{4+} giving square pyramidal complex. In VH-SAPO-34, only one ethanol is found to coordinate with the VO^{2+}.[11] It has been suggested that two methanol coordinate with Cu^{2+} ions in CuH-SAPO-11.[19]

For C_3H_7OD adsorption, the best fit is for interaction with one propanol molecules at a VO^{2+}-D distance of 4.2 Å. InVH-SAPO-34, only one propanol is found to coordinate with the VO^{2+}.[11] Fig. 9. shows similar structure to adsorbed ethanol.

When we compare the ESR parameters of methanol, ethanol or propanol adsorbed VH-SAPO-11 with water adsorbed VH-SAPO-11, we find some notable differences. G values is somewhat larger for the water sample adsorbed. These differences propose that the water-VO^{2+} complex has a geometry in VH-SAPO-11 different from that of methanol,. ethanol, propanol-VO^{2+} complex.

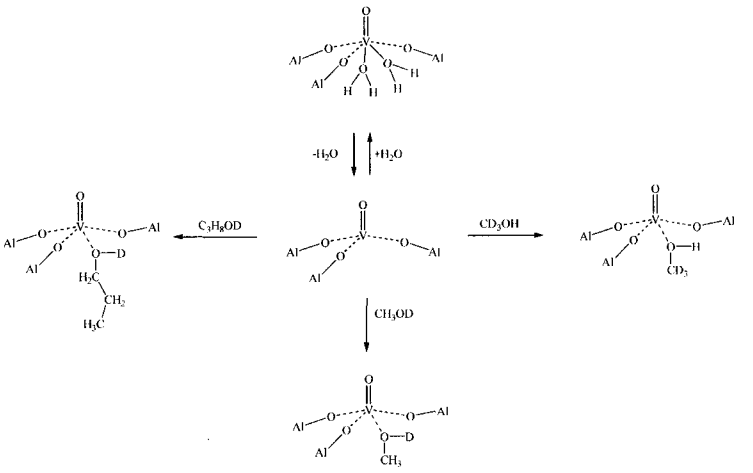

Fig. 9. Proposed model structures for various vanadium-adsorbate complexes in VH-SAPO-11.

CONCLUSIONS

Electron spin echo modulation spectroscopy, when coupled with electron spin resonance spectroscopy, has been shown to be very effective for obtaining information about the nature and location of vanadium in VH-SAPO-11 and in also its coordination behavior toward various adsorbates. Species A is proposed as a $VO(H_2O)_3^{2+}$ complex coordinated to three framework oxygens. The majority of VO^{2+} ions in a fully dehydrated H-SAPO-11 are situated in site I, the center of double 6-ring that form a 6-ring channel. During calcinations, part of the v^{4+} ions are oxidized to v^{5+}. Calcined, hydrated VH-SAPO-11 after dehydration at elevated temperature shows a new vanadium species B, which is suggested to be VO^{2+} ion with no water or hydroxyl ligands. Adsorption of D_2O on dehydrated VH-SAPO-11 regenerates species A and is suggested from the ESR spectrum as $VO(D_2O)_2$ with vanadium coordination of the type $(VO)O_2(O_f)_3$ where O_f is a framework oxygen. Adsorption of deuterated methanol on dehydrated VH-SAPO-11 generates another new vanadium species

D, which is identified as $VO(CD_3OH)^{2+}$ with vanadium coordination of the form $(VO)O(O_f)_3$. When deuterated ethanol is adsorbed on dehydrated VH-SAPO-11; a new vanadium species E identified as $VO(C_2H_5OD)^{2+}$. When deuterated propanol is adsorbed on dehydrated VH-SAPO-11; a new vanadium species F identified as $VO(C_3H_7OD)^{2+}$ with VO^{2+} - weak adsorbate interaction. Adsorption of polar molecules such as water, methanol, ethanol, and propanol induces the migration of VO^{2+} ions to site II_1^*, close to 6-ring that forms a window of the 10-ring cannel where adsorbates can directly coordinate with VO^{2+}.

Acknowledgements

This research financially supported by the Changwon National University in 2004.

REFERANCES

1. S. T. Wilson, B. M. Lok, C. A. Messina, T. R. Cannon and E. M. Flanigen, *J. Am. Chem. Soc.* **104**, 1146 (1982).
2. B. M. Lok, C. A. Messina, R. L. Patton, R. T. Gajek, T. R. Cannon and E. M. Flanigen, *J. Am. Chem. Soc.* **106**, 6092 (1984).
3. M. –A. Dijeugou, A. Prakash, and L. Kevan, *J. Phys. Chem.* B **103**(No. 5) 804-811 (1999).
4. M. Hartmann, N. Azuma, and L. Kevan, *J. Phys. Chem.* **99**, 10988 (1995).
5. M. Hartmann, N. Azuma, and L. Kevan, In Zeolites, "A refined Tool for Designing Catalytic Sites" L. Bonneviot, and S. Kaliaquinee Eds., Elsevior, New York, 335 (1995).
6. A. M. Prakash, M. Hartmann, and L. Kevan, *J. Chem. Soc., Faraday Trans.* **93**, 1233 (1997).
7. G. Bellussi, and M. S. Rigutto, "Advanced Zeolite Science and Application" J. C. Jansen, M. Stoker, H. G. Karge, and J. Weitkamp, Eds., "Studies in Surface Science and Catalysis 85", Elsevier, Amsterdam,177-213 (1994).
8. A. Miyamoto, D. Medhanavayn, and I. Inui, *Appl. Catal. 28*, 89, (1986).
9. T. Blaso, P. Concepeion, J. M. Lopez Nieto, and J. Perez-Pariente, *J. Catal.* **152**, 1 (1995).
10. Puyam So Singh, Rjib Bandyopadhyah, and B. S. Rao, *J. Molecular Catal. A : Chemical* **104**(1) 103-10 (1995).
11. G. Back, Y.-S. Cho, Y.-I. Lee, Y. Kim, and L. Kevan, *J. Kor. Mag. Res. Soc.* **5**, 73-90 (2001).
12. L. Kevan, "Time domain Electron Spin Resonance" L. Kevan, and R. N. Schwarz, Eds., Wiley New York 1979 Chap 9, S. A. Dikanov, A. A. Shubin, and V. N. Parmon, *J. Mag.*

Res. **42**, 474 (1981).
13. C. Zhixiang, K. Rajit, R. M. Krishna and L. Kevan, *J. Phys. Chem.* B **104**, 5579 (2000).
14. A. Ojo and L. McCusker, *Zeolites*, **11**, 460 (1991).
15. C. Monte, M. E. Davis, B. Murray, and M. Narayana, *J. Phys. Chem.* **94**, 6431 (1990).
16. M. S. Riguta, and H. J. van Beckkum, *J. Mol. Catal.* **81**, 77 (1993).
17. B. M. Weckhuyson, I. P. Vannijvel, and R. A. Schoonheydt, *Zeolites*, **15**, 482 (1995).
18. A. M. Prakash and L. Kevan, *J. Phys. Chem.* **103**, 2214 (1999).
19. C. W. Lee, X. Chen, and L. Kevan, *J. Phys. Chem.* **95**, 8626 (1991).
20. G. Centi, J. R. Wasson, F. Trifiro, A. Aboukais, C. F. Aissi, and M. Guelton, *J. Phys. Chem.* **100**, 15947 (1996).
21. J-S. Yu, and L. Kevan, *Langmuir*, **1**, 1617 (1995).
22. I. Siegel, *Phys. Rev.*, **134**, A193-7 (1964).
23. Ballutaud D, D. Bordes E. and Courtine P. *Mater. Res. Bull.*, **17**, 519-26 (1982).
24. Ballutaud D, Bordes E. and Schinder R. N., *Z. Naturf.*, **36a**, 992-5 (1981).
25. M. Narayana, C. S. Narashimhan and L. Kevan, *J. Chem. Soc., Faraday Trans.*, **81**, 137 (1985).
26. E. Servica and R. N. Schindler *Z. Naturf.* **36a**, 992 (1981).
27. C. W. Lee, J.-S. Yu and L. Kevan *J. Phys. Chem.* **96**, 7747 (1992).